

Theoretical Description of Scanning Tunneling Potentiometry

Weigang Wang(王魏刚)* and Malcolm R. Beasley
*Geballe Laboratory for Advanced Materials,
Stanford University, Stanford, CA 94305*
(Dated: May 29, 2022)

A theoretical description of scanning tunneling potentiometry (STP) measurement is presented to address the increasing need for a basis to interpret experiments on macroscopic samples. Based on a heuristic understanding of STP provided to facilitate theoretical understanding, the total tunneling current related to the density matrix of the sample is derived within the general framework of quantum transport. The measured potentiometric voltage is determined implicitly as the voltage necessary to null the tunneling current. Explicit expressions of measured voltages are presented under certain assumptions, and limiting cases are discussed to connect to previous results. The need to go forward and formulate the theory in terms of a local density matrix is also discussed.

PACS numbers: 07.79.-v,72.10.Bg,73.23.-b,73.50.-h

I. INTRODUCTION

The use of scanning probes is now widespread. However, very few of these probes measure transport at very short length scales. The ultimate probe for such measurements is scanning tunneling potentiometry (STP)^{1,2}, in which a scanning tunneling microscope (STM) is used to measure the local potential due the flow of an applied current. However, only recently have we and others developed STP instruments that can routinely make measurements under a wide range of conditions and essentially at the fundamental noise limit of STP.³⁻⁶

With our STP, we have focussed on local quantum transport in macroscopic materials, as distinct from quantum transport through nanostructures (e.g., single molecules, nanotubes and lithographically produced nanostructures). Our work demonstrates that potential maps can be obtained in appropriate materials down to distances smaller than all the length scales relevant in transport (the inelastic scattering length, the elastic scattering length and even the Fermi wave length). An example of an STP image on these very short length scales obtained in our laboratory is shown in Figure 1 for an epitaxial graphene sample. As can be seen in the figure, there is considerable local structure in the potential that is relatively large in magnitude. It is the lack of a quantitative basis for interpreting such images that motivates this paper. We hope both to explain the theoretical issues for experimentalists and to motivate the needed theoretical extensions for theorists.

There are two issues. First, it is not clear exactly what potential is being measured. Macroscopically, the measured potential would be the usual local electrochemical potential. However, at such short length scales as STP probes, one cannot use thermodynamic concepts. Second, the situation is inherently quantum mechanical and any calculation of the potential must include the underlying quantum mechanical processes.

These issues are not entirely new. To some degree they have been addressed in the theories relevant to transport through nanostructures where the sample is small

compared to characteristic lengths of the transport. On the other hand, in the case of these nanostructures, in most of the cases the measurement contacts are relatively macroscopic (compared with an STP tip), and cannot be scanned. Moreover, the interfaces between the contacts and the sample play an important role in the overall transport. Numerous theories have been developed to deal with this situation. Some of them also consider what an STP would measure inside a nanostructure⁷⁻¹¹, although there are no existing STP data yet that can be compared with these theories. In any event, regarding the specific question of what STP measures, it was possible to write down explicit expressions for the STP voltage (for example, see equation (37) of reference 7). On the other hand, these expressions are explicitly dependent on the voltages applied on the current leads. By contrast, in the case where the sample is macroscopically large, the geometry and microscopic processes present in the leads obviously cannot matter. Hence a proper theoretical formulation is required, and precisely what STP measures remains unclear.

In this paper, we take some first steps toward a theoretical description of a STP measurement of local quantum transport in a macroscopic sample. The relevant quantum mechanical quantity is the density matrix, and it is possible to develop an implicit (and under some approximations, an explicit) relation from which the measured potential can be determined in terms of the density matrix and the tunneling process into the sample. While the tunneling process associated with the STM tip can be accounted for, it is a separate matter how to do the calculation of the density matrix under the relevant nonequilibrium conditions and short length scales in a macroscopic sample. We do not address these computational challenges in this paper. As stated above, our goal is to understand scanning tunneling potentiometry in terms accessible to experimentalists and to define the deeper theoretical questions needing attention. Toward these ends, we use both heuristic and more formal approaches. More specifically, in the formal development, our results pose new problems in quantum transport that

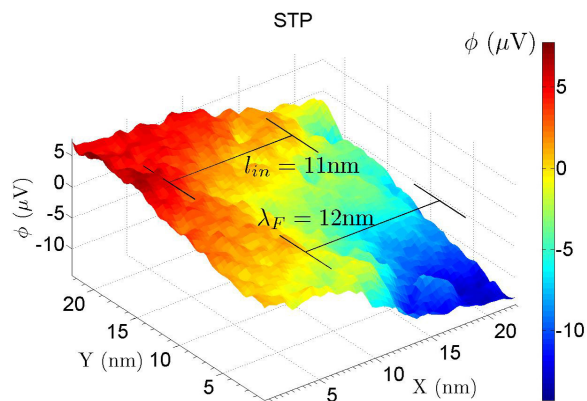


FIG. 1. STP data taken on epitaxial graphene as an example of transport measurement at length scales smaller than all the length scales relevant in the transport. As seen in the figure, on top of the average gradient, STP shows variations on the nanometer length scale.

need proper theoretical attention in order to have a complete theory suitable for interpreting experiment. One example is the need for formulations in terms of local density matrices as opposed to global ones.

We note that some of the issues discussed above have been addressed by Chu and Sorbello¹² in the context of their calculation of the residual resistivity dipole of a scattering center in the spirit of Landauer¹³. As noted in their paper, the potential measured in STP is not the same as the local electrostatic potential in the material generated by an electric current. Our work can be thought of as a generalization of their work and an articulation more from the general point of view of a theory of STP measurement. Compared to Chu and Sorbello, our result is more general; and in the final result, instead of a weighted sum, we obtained a form which consists of matrices either being density matrix of the sample or defined with sample and tip wave functions.

This paper is organized as follows. First, we describe the setup for STP measurement, also serving to emphasize that what is operationally measured is the potential necessary to achieve zero current through the potentiometric contact. We provide a heuristic understanding of STP measurement in general terms. Next, we present a simple model of only two scattering centers with mesoscopic distance to motivate a more general theory. This leads naturally to the use of the density matrix of the sample in the expression of the tunneling current detected in STP and thereby gives meaning to what is being measured. After that, we discuss the need to use a local density matrix in the case of macroscopic samples. Finally, we discuss several limiting cases of our theory to illustrate better its physical content.

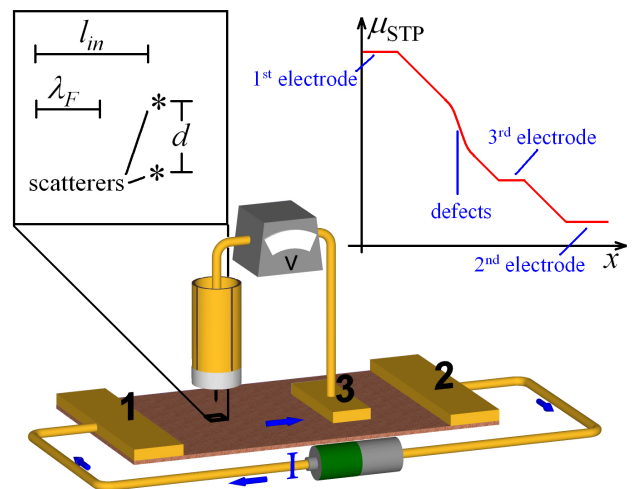


FIG. 2. Schematic setup of scanning tunneling potentiometry, and model problem to be considered in this paper. Electrodes 1, 2 and 3 are macroscopic contacts, while the STM tip, microscopically connected to the sample, functions as the fourth electrode. The sample is macroscopic in size and STP probes a small region which is enlarged to the upper left. The region has two scattering centers, and the rest of the sample is assumed to be homogeneous and defect-free, with no defects (scatterers) present. The distance between the two defects, the Fermi wavelength and the inelastic mean free path of the sample are all comparable. To the upper right presents an expected STP result on a large length scale, including the electrodes.

II. SCANNING TUNNELING POTENTIOMETRY

A. STP setup

As seen in Figure 2, STP is effectively a four-point transport measurement using an STM tip. In an STP measurement, a floating current source provides a current through the sample via electrodes 1 and 2; a voltage is applied between the third electrode and the STM tip, which serves as the fourth electrode. The voltage is so adjusted that the tunneling current between the sample and the STM tip is zero – the definition of a potentiometric measurement. This applied voltage which nulls the tunneling current is the data that is recorded in an STP measurement. Moreover, the capability of STM to scan on nanometer scales makes STP measurement a nanoscale transport measurement. The outcome of the experiment is in the form of a potential map of the scanning area accompanied by a topographical map (obtained by conventional STM operation) of the same area taken point by point successively with the potential (see Ref 3 for details).

B. A heuristic interpretation of STP

Now consider a macroscopic sample where the current contacts are far removed, specifically where the sample size and the distance between the current contacts are large compared to characteristic transport length scales. Our goal is to address the question what STP really measures under these conditions. This measured value in STP would correspond to the local electrochemical potential in the thermodynamic limit (i.e., a large distance between the voltage measurements and a large voltage contact area in addition to a macroscopic sample size). In STP the situation is more subtle.

In a conventional STM measurement, the total tunneling current is written¹⁴:

$$I = \frac{4\pi e}{\hbar} \sum_{\vec{k}, \vec{k}'} [f_s(\vec{k}) - f_t(\vec{k}')] \delta(E_{sc, \vec{k}} - eV_s, E'_{tc, \vec{k}'} - eV_t) |M|^2, \quad (1)$$

where $\delta(E_1, E_2)$ is the Kronecker delta symbol, f_i ($i = s, t$) are Fermi-Dirac distribution functions of the sample and the tip, respectively; $|M|^2$ is the magnitude of tunneling matrix elements, which are assumed to be constant in this equation; $E_{ic, \vec{k}}$ are eigen energies of the specific states of the sample and the tip, where the energies here are measured with respect to the band (“chemical energy”, see Figure 3 for clarifying definitions of chemical energy, electrostatic energy and the sum of these two, the electrochemical energy); and $-eV_i$ are the energies associated to the electrostatic potential in the sample and the tip (“electrostatic energy”, also see Figure 3).

Two modifications need to be made in order to use the form of equation (1) in the case of a potentiometric transport measurement. First, the distribution function of the sample is not one in equilibrium due to existence of an applied current through the sample, and hence is not a Fermi-Dirac distribution. And second, the magnitude of tunneling matrix elements $|M|^2$ should not be assumed as a constant for each tunneling channel, hence in the expression one should use an equivalent average value for the magnitude of tunneling matrix elements.

Consider now an example of the distribution function in a non-equilibrium transport situation. In the linear response region of a homogeneous sample with no defects

and only inelastic scattering with mean free path l_{in} , the set of electrons with a certain direction of wave vector is described by an effective chemical potential dependent on this direction¹², i.e., $f_s(\vec{k}) \propto (e^{\beta(E - \mu_{\hat{\theta}})} + 1)^{-1}$ (here $\beta \equiv 1/(k_B T)$, see also Section V). A distribution function $f_s(E_{s, ec})$ can be defined as the average probability of occupancy for each energy $E_{s, ec}$, where the averaging runs over all degenerate states (with different direction of wave vector, for example). Plotting $f_s(E_{s, ec})$ as a function of $E_{s, ec}$, it is expected that $f_s \approx 1$ at low energy and $f_s \approx 0$ at high energy, but in the transition region between low and high energies, it is not a Fermi-Dirac distribution. If we ignore the broadening of the distribu-

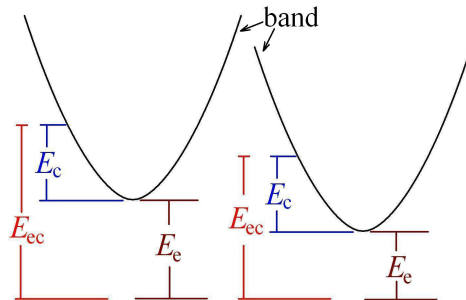


FIG. 3. Definitions of different energies in the problem. Chemical energies (E_c) are defined with respect to the band, e.g., the band bottom; electrostatic energies (E_e) are energy differences associated with the band bending due to existence of an electrostatic field; and the sum of these two energies are the electrochemical energies (E_{ec}). Electrons at different positions of the sample with the same chemical energy and wave vector have the same wave function, while they do not necessarily have the same electrochemical energy due to band bending. Although electrochemical energy is the appropriate energy one needs to use when comparing energies at different positions, it is easier to keep track of quantum states with chemical energies.

tion function due to finite temperature, with a constant current and a cylindrical Fermi surface, in the previous case where the sample is homogeneous and defect-free, the distribution function is in the form (see also Figure 4 for more detailed clarification):

$$f_s(E_{s, ec}) = \begin{cases} 1 & E_{s, ec} < \mu - el_{in}E_0 \\ 1 - \frac{(el_{in}E_0 - \mu + E_{s, ec})^{3/2}}{2(el_{in}E_0)^{3/2}} & \mu - el_{in}E_0 < E_{s, ec} < \mu \\ \frac{(el_{in}E_0 + \mu - E_{s, ec})^{3/2}}{2(el_{in}E_0)^{3/2}} & \mu < E_{s, ec} < \mu + el_{in}E_0 \\ 0 & E_{s, ec} > \mu + el_{in}E_0 \end{cases} \quad (2)$$

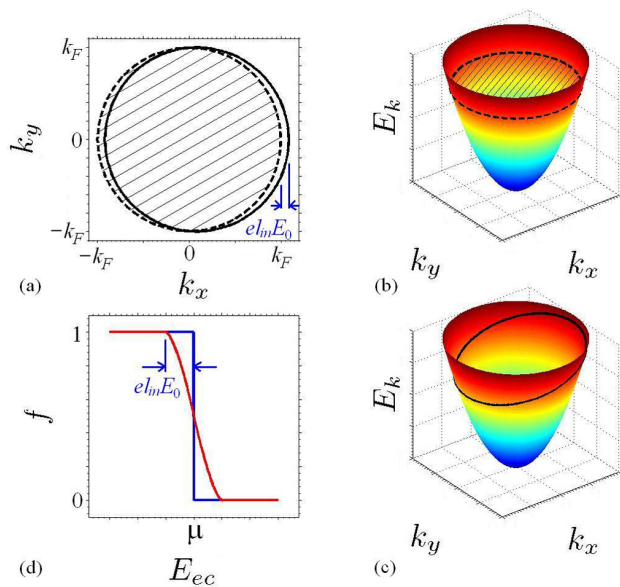


FIG. 4. Comparison of distribution functions with and without current. (a) When there is a current, the equilibrium Fermi surface (dashed line and shaded) is shifted to the right (solid line). (b) When viewed in the $E-\vec{k}$ diagram, in equilibrium, the Fermi surface is a horizontal circle, (c) while when current exists, the Fermi surface is tilted. (d) The occupation rate for each energy, i.e., the distribution function (solid red curve), is different than Fermi-Dirac distribution (blue curve). The distribution function in more complicated situations, for example, when elastic scattering exists, is expected to be different and more interesting than illustrated here.

where E_0 is the electric field and l_{in} is the inelastic mean free path.

Comparing the distribution function of the sample to that of the tip (a Fermi-Dirac distribution), it is clear that electrons with relatively low energies will tend to flow from the tip to the sample, and electrons with relatively high energies will tend to flow in the opposite direction. Hence the total tunneling current is a weighted sum of the difference of the two distribution functions. The weight for each energy is clearly related to the density of states, however, this weight is also related to the tunneling matrix elements as they are determined by wave function values at a certain position (tip center of curvature) and should not be assumed to be the same as in equation (1). One can write:

$$I = \frac{4\pi e}{\hbar} \int_{-\infty}^{\infty} [f_s(\epsilon) - f_t(\epsilon - eV_t)] N_s(\epsilon) N_t(\epsilon - eV_t) \overline{|M|^2} d\epsilon, \quad (3)$$

where V_t , which is the voltage on the tip, effectively moves the distribution function f_t (blue curve in Figure 4(d)) in the horizontal direction, such that the total tunneling current equals zero. Here, the densities of states are more or less semi-classical while the average mag-

nitude of the tunneling matrix represents the quantum interference, which we will study in detail in next section. This concept that the total current is proportional to a weighted sum of the difference of two distribution functions is not unlike thermal electric effect, although in that case it is the difference in temperature that is the origin of the difference in distribution function, while in our case it is the nonequilibrium nature of current flow.

From equation (3) it is clear that STP does not measure a well defined thermodynamic potential, rather, it measures the non-equilibrium distribution function of the sample with the weight for each energy due to both densities of states and quantum interference effects in the tunneling matrix. To actually calculate this weight, a density matrix is needed, which is described below. It is also clear that even with the same distribution function, due to relative change in the tunneling matrix element from quantum interference from one measurement point to another, the STP voltage can change. This accounts for the STP fluctuation in Chu & Sorbello's paper¹². The basic message of this heuristic consideration is that the STP potential reflects both changes in the distribution functions and the tunneling matrix elements as a function of position. These insights provide a qualitative basis for considering experiment and set the stage for a more exact theoretical treatment.

III. GENERAL THEORY IN TERMS OF DENSITY MATRIX

A. Simple model considered in the problem

We introduce a simple model presented in Figure 2, to represent a macroscopic sample with defects closer to one another than the inelastic mean free path. In the problem, the sample is macroscopic and connected to the current providing electrodes macroscopically. The STM tip probes a small region on the sample, and inside this small region are two scattering centers near each other. The rest of the sample is assumed to be defect-free and homogeneous, with inelastic mean free path l_{in} and Fermi wavelength λ_F . These two parameters are both comparable to the distance between the two defects in the problem. The electrochemical potential on the sample is expected to be a linear curve with respect to position except for where the defects are, as also shown in the figure. However, as one expects from physical consideration, and explained in detail below, when comparing STP data taken at nearby points, such thermodynamic concepts are inadequate.

In this problem, one can ask the following two questions: a) what is the STP measurement result near the two defects? b) what is the cross section of the two defects, if seen far away and treating them as one single defect? The answer to the second question determines STP measurement result far away from the defects, as in that case STP measures the Landauer resistive dipole

potential¹³. One needs to solve a similar problem to answer both questions.

B. Quantum transport approach

In the quantum transport approach¹⁵, one uses a density matrix¹⁶ to describe the sample, and treat all three contacts as electron reservoirs that have Fermi-Dirac distributions. The necessity of density matrix in solving the model problem posed above can be appreciated with the following consideration, with plane waves as the basis set for electron wave functions:

Suppose we start with an incident plane wave. The plane wave will be scattered by either of the two defects. The scattered wave is coherent with the incident wave. As it propagates, the magnitude of the coherent part shrinks due to inelastic scattering, which generates waves having indefinite phase difference with the incident and scattered waves. Moreover, the scattered coherent wave can be scattered by the other defect, generating a coherent secondary scattered wave. In short, the incident plane wave will be scattered back and forth by both scattering centers, with decaying coherent part. In addition, the incoherent waves generated by inelastic scattering will individually also be scattered back and forth and generate coherent sets of their own. The situation which combines coherence from elastic scattering and incoherence and probability from inelastic scattering is formally described by a density matrix. The density matrices resulting from all the incident plane waves which are incoherent to one another should be added to obtain the net density matrix.

In this paper, we do not undertake the calculation of the density matrix of the sample. Rather, we assume that the density matrix has been calculated. We did include the macroscopic contacts in the problem, since they are needed in determining the density matrix of the sample in the Non Equilibrium Green Function-Landauer approach¹⁵. The objective of this paper is to calculate the total tunneling current based on the density matrix of the sample and properties of the STM tip. Once the total tunneling current is obtained with the voltage applied on the tip as a parameter, by setting that current to zero one implicitly determines STP measurement result.

C. Total tunneling current

In calculating the total tunneling current, we have the density matrix of the sample, denoted by $\hat{\rho}$, and describe the STM tip with a Fermi-Dirac distribution function:

$$f(E_{c,\bar{p}} - eV_t - \mu) = \frac{1}{e^{\beta(E_{c,\bar{p}} - eV_t - \mu)} + 1},$$

with $\{|\chi_{\bar{p}}\rangle\}$ as its basis set. Here V_t is the voltage applied on the STM tip, $E_{c,\bar{p}}$ is the chemical eigen energy of state $|\chi_{\bar{p}}\rangle$, and μ is the electrochemical potential of the tip.

To derive the expression for the total tunneling current, we start by diagonalizing the density matrix $\hat{\rho}$ of the sample. After diagonalization, the density matrix reads:

$$\hat{\rho}_\psi = \begin{pmatrix} \ddots & & \dots & & \dots \\ & \rho_{\psi\bar{k}\bar{k}} & & 0 & \\ \vdots & & \ddots & & \vdots \\ & 0 & & \rho_{\psi\bar{k}'\bar{k}'} & \\ \dots & & \dots & & \ddots \end{pmatrix}, \quad (4)$$

where $\rho_{\psi\bar{k}\bar{k}} = \langle \psi_{\bar{k}} | \hat{\rho} | \psi_{\bar{k}} \rangle$. Here we use $\hat{\rho}$ for the abstract density matrix, and use $\hat{\rho}_\psi$ for the matrix form of the density matrix under the basis set $\{|\psi_{\bar{k}}\rangle\}$. In this particular case, this basis set diagonalizes the density matrix.

The basis set $\{|\psi_{\bar{k}}\rangle\}$ consists of wave functions that are incoherent to each other in the problem, and the diagonal elements in the density matrix $\hat{\rho}_\psi$ have physical meanings that the probability of finding an electron in state $|\psi_{\bar{k}}\rangle$ is $\rho_{\psi\bar{k}\bar{k}}$. Note that elastic scattering only scatters states with a given eigen electrochemical energy into states with the same eigen electrochemical energy, thus one can choose $\{|\psi_{\bar{k}}\rangle\}$ such that they are all energy eigen states, with $E_{ec,\bar{k}}$ as their eigen electrochemical energies. Since we are using chemical energies for states in the tip and electrochemical energies for states in the sample, the subscripts ‘‘s’’ and ‘‘t’’ in the denotation of energy levels for sample and tip have been omitted.

As shown in Figure 5, the tunneling current between one state $|\psi_{\bar{k}}\rangle$ of the sample and one state $|\chi_{\bar{p}}\rangle$ of the tip is calculated through evaluating a surface integral over Σ between the sample and the tip, and reads¹⁴:

$$I_{\bar{k},\bar{p}} = \frac{4\pi e}{\hbar} [\rho_{\psi\bar{k}\bar{k}} - f(E_{c,\bar{p}} - eV_t - \mu)] \delta(E_{ec,\bar{k}}, E_{c,\bar{p}} - eV_t) \times \left(\frac{\hbar^2}{2m} \right)^2 \left| \int_{\Sigma} (\psi_{\bar{k}} \vec{\nabla} \chi_{\bar{p}}^* - \chi_{\bar{p}}^* \nabla \psi_{\bar{k}}) \cdot d\vec{S} \right|^2. \quad (5)$$

The tunneling current resulting from different channels are additive, because both the states of the sample and the states of the tip are incoherent with one another. Thus the total tunneling current is:

$$I = \sum_{\bar{k},\bar{p}} \left\{ \frac{4\pi e}{\hbar} [\rho_{\psi\bar{k}\bar{k}} - f(E_{c,\bar{p}} - eV_t - \mu)] \delta(E_{ec,\bar{k}}, E_{c,\bar{p}} - eV_t) \times \left(\frac{\hbar^2}{2m} \right)^2 \left| \int_{\Sigma} (\psi_{\bar{k}} \vec{\nabla} \chi_{\bar{p}}^* - \chi_{\bar{p}}^* \nabla \psi_{\bar{k}}) \cdot d\vec{S} \right|^2 \right\} \quad (6)$$

The tunneling matrix element:

$$M_{\bar{k}\bar{p}} \equiv \delta(E_{ec,\bar{k}}, E_{c,\bar{p}} - eV_t) \frac{\hbar^2}{2m} \int_{\Sigma} (\psi_{\bar{k}} \vec{\nabla} \chi_{\bar{p}}^* - \chi_{\bar{p}}^* \nabla \psi_{\bar{k}}) \cdot d\vec{S} \quad (7)$$

can be written in another way if one expands the wave function of the tip into spherical harmonics (see chapter 3.2 of reference 14):

$$\chi_{\vec{p}}(\vec{r}) = \sum_{l,m} C_{lm,\vec{p}} k_l(\kappa\rho) Y_{lm}(\theta, \phi), \quad (8)$$

where besides the familiar denotation of Y_{lm} as the spherical harmonic functions, k_l is the l^{th} spherical modified Bessel function of the second kind. There exists a general derivative rule (chapter 3.4 of reference 14) that the density matrix element (7) can be written as a linear operation of the sample state only, evaluated at the center of curvature \vec{r}_0 of the tip which is also the origin for expanding the tip wave functions:

$$M_{\vec{k}\vec{p}} = (\mathcal{F}_{(\vec{p},V_t)}\psi_{\vec{k}}) |_{\vec{r}_0}. \quad (9)$$

For instance, if the tip wave function is well approximated by a s -wave, then:

$$\mathcal{F}_{(\vec{p},V_t)} = \frac{2\pi C_{\vec{p}} \hbar^2}{\kappa m} \delta(E_{ec,\vec{k}}, E_{c,\vec{p}} - eV_t),$$

which is a pure number. As another example, for a p_z -wave tip state, one has:

$$\mathcal{F}_{(\vec{p},V_t)} = \frac{2\pi C_{\vec{p}} \hbar^2}{\kappa m} \delta(E_{ec,\vec{k}}, E_{c,\vec{p}} - eV_t) \frac{\partial}{\partial z}.$$

When the pure state $\chi_{\vec{p}}$ is a combination of the s , p , d \dots waves, the corresponding operators are additive.

The total tunneling current can be expressed:

$$I = \sum_{\vec{k},\vec{p}} \frac{4\pi e}{\hbar} [\rho_{\psi_{\vec{k}\vec{k}}} - f(E_{c,\vec{p}} - eV_t - \mu)] \left| (\mathcal{F}_{(\vec{p},V_t)}\psi_{\vec{k}}) |_{\vec{r}_0} \right|^2, \quad (10)$$

where the Kronecker delta symbol has been absorbed in the operator $\mathcal{F}_{(\vec{p},V_t)}$, and these operators are well defined only between energy eigen states. From the point of view of the heuristic approach in Section II, $\rho_{\psi_{\vec{k}\vec{k}}}$ serves as the distribution function, and $\left| (\mathcal{F}_{(\vec{p},V_t)}\psi_{\vec{k}}) |_{\vec{r}_0} \right|^2$ serves as the magnitude of tunneling matrix element, and the averaging of the tunneling matrix element is effectively defined such that equation (3) equals equation (10). Note that the densities of states of both the sample and the tip have been reflected in the summation over all states of the tip and all states of the sample.

The above expression for the total tunneling current requires diagonalization of the density matrix of the sample. To obtain an abstract expression, one needs to rewrite it into a form which is a product of a matrix with the density matrix of the sample. When only states that are electrochemical energy eigen states are used in the basis sets, say $\{|\phi_{\vec{k}}\rangle\}$, with density matrix of the sample in the form:

$$\hat{\rho}_\phi = \begin{pmatrix} \ddots & & \dots & & \dots & & \\ & \rho_{\phi_{\vec{k}\vec{k}}} & & \rho_{\phi_{\vec{k}\vec{k}'}} & & & \\ \vdots & & \ddots & & \vdots & & \\ & \rho_{\phi_{\vec{k}'\vec{k}}} & & \rho_{\phi_{\vec{k}'\vec{k}'}} & & & \\ \dots & & \dots & & \ddots & & \end{pmatrix}, \quad (11)$$

this matrix-product form of the expression is:

$$I = \sum_{\vec{p}} \frac{4\pi e}{\hbar} \text{tr} \left[\vec{\phi}_0^\dagger \vec{\phi}_0 [\hat{\rho}_\phi - f(E_{c,\vec{p}} - eV_t - \mu)] \right] = \frac{4\pi e}{\hbar} \text{tr} \left[\left(\sum_{\vec{p}} \vec{\phi}_0^\dagger \vec{\phi}_0 \right) \hat{\rho}_\phi - \left(\sum_{\vec{p}} f(E_{c,\vec{p}} - eV_t - \mu) \vec{\phi}_0^\dagger \vec{\phi}_0 \right) \right], \quad (12)$$

where:

$$\vec{\phi}_0 = (\mathcal{F}_{(\vec{p},V_t)}\phi_{\vec{k}_1}(\vec{r}_0), \dots, \mathcal{F}_{(\vec{p},V_t)}\phi_{\vec{k}_i}(\vec{r}_0), \dots, \mathcal{F}_{(\vec{p},V_t)}\phi_{\vec{k}_n}(\vec{r}_0)). \quad (13)$$

Here, the order of stacking $\phi_{\vec{k}}$'s for the symbols $\vec{\phi}_0^\dagger$ and $\vec{\phi}_0$ is the same as that was adopted in writing the density matrix $\hat{\rho}_\phi$. Note that the wave functions in the basis set $\{|\phi_{\vec{k}}\rangle\}$ are all electrochemical energy eigen functions, which makes $\mathcal{F}_{(\vec{p},V_t)}$ well defined.

Although the above results are explicitly written down

with the basis set $\{|\phi_{\vec{k}}\rangle\}$ which includes only energy eigen functions, one does not need this eigen function requirement. The matrices $\sum_{\vec{p}} \vec{\phi}_0^\dagger \vec{\phi}_0$ and $\sum_{\vec{p}} f(E_{c,\vec{p}} - eV_t - \mu) \vec{\phi}_0^\dagger \vec{\phi}_0$ have the same transformation rules as other operators (and density matrices) in the Hilbert space. Under other basis sets, in general one does not have an explicit

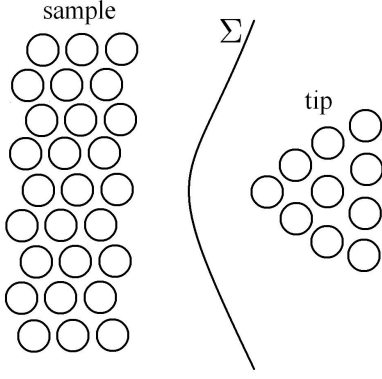


FIG. 5. Calculation of the tunneling current. The tunneling matrix element between one state of the sample and one state of the tip is evaluated by a surface integration over the surface Σ between the sample and the tip (see equation (5)). Refer to reference 14 for details. This figure is redrawn in complete analogy to Figure 3.1 in this reference. Here the circles represent atoms of the sample (left) or the tip (right), and the surface Σ is an imaginary surface in vacuum over which the integration in equation (5) is performed.

expression that links the matrix elements to the value of the sample wave function at a certain point (except for the special case discussed shortly in next subsection).

In equation (12), the tip and sample properties are en-

tangled by the δ -symbols, and we were not able to find an explicit expression for the measured STP potential μ although it is implicitly defined by setting equation (12) to be zero. We now introduce some further simplifications that make explicit expressions possible.

D. Explicit expressions for measured potential

In this subsection we assume that the tip is featureless, in the sense that: a) the tip has a uniform density of states N_t over the energy range that we are interested in; and b) the operator defined in equation (9) equals:

$$\mathcal{F}_{(\vec{p}, V_t)} = \delta(E_{ec, \vec{k}}, E_{c, \vec{p}} - eV_t) \mathcal{F}_0, \quad (14)$$

i.e., the \vec{p} dependence is only in the δ -symbol.

Under the above simplifications, in equation (12) the sum over \vec{p} can be explicitly carried out and one obtains:

$$\sum_{\vec{p}} \vec{\phi}_0^\dagger \vec{\phi}_0 = N_t \vec{\phi}_{00}^\dagger \vec{\phi}_{00}, \quad (15)$$

$$\sum_{\vec{p}} f(E_{c, \vec{p}} - eV_t - \mu) \vec{\phi}_0^\dagger \vec{\phi}_0 = N_t \vec{\phi}_{00}^\dagger \vec{\phi}_{00} \hat{\rho}_{\phi, FD}(\mu), \quad (16)$$

where:

$$\vec{\phi}_{00} = (\mathcal{F}_0 \phi_{\vec{k}1}(\vec{r}_0), \dots, \mathcal{F}_0 \phi_{\vec{k}i}(\vec{r}_0), \dots, \mathcal{F}_0 \phi_{\vec{k}n}(\vec{r}_0)), \quad (17)$$

$$\hat{Q}_{FD}(\mu) = \frac{1}{1 + e^{\beta(\hat{H}_s - \mu)}}, \quad (18)$$

and \hat{H}_s is the Hamiltonian of the sample.

Note that the above equations are basis-transformation-independent, hence we do *not* require the basis wave functions to be energy eigen functions for the expressions in this subsection. The matrix form of the total tunneling current is then:

$$I = \frac{4\pi e}{\hbar} N_t \cdot \text{tr} \left[\vec{\phi}_{00}^\dagger \vec{\phi}_{00} (\hat{\rho}_\phi - \hat{\rho}_{\phi, FD}(\mu)) \right], \quad (19)$$

It is noteworthy to compare the above equation to equation (3). One can immediately see the resemblance of the two equations, except that the density of states of the sample is implicitly included in the summation of the trace operation. One can also see that it is the difference of the density matrix that STP measures (with a weight), thus in order to express things in terms of effective distribution functions, a mean matrix element value should be used and that value is expected to change over space (as seen in the definition of $\vec{\phi}_{00}$ in equation (17)).

a. Subcase I In this subcase, we consider a situation where temperature is high compared to deviations

from thermal equilibrium due to the applied current. For example, in Figure 4 for the heuristic understanding of STP, we need to have $k_B T \gg e l_{in} E_0$, rather than a sharp transition in distribution function implying $T \approx 0$. We assume the density matrix is very close to the thermal equilibrium with electrochemical potential μ_0 , and measured STP potential is $\mu_0 + \Delta\mu$, then:

$$\begin{aligned} & \text{tr} \left[\vec{\phi}_{00}^\dagger \vec{\phi}_{00} (\hat{\rho}_\phi - \hat{\rho}_{\phi, FD}(\mu_0)) \right] \\ &= \text{tr} \left[\vec{\phi}_{00}^\dagger \vec{\phi}_{00} (\hat{\rho}_{\phi, FD}(\mu_0 + \Delta\mu) - \hat{\rho}_{\phi, FD}(\mu_0)) \right] \end{aligned} \quad (20)$$

Noticing:

$$\begin{aligned} & \frac{1}{1 + e^{\beta(E - \mu_0 - \Delta\mu)}} - \frac{1}{1 + e^{\beta(E - \mu_0)}} \\ & \approx \frac{\beta}{2 + e^{-\beta(E - \mu_0)} + e^{\beta(E - \mu_0)}} \Delta\mu, \end{aligned}$$

we get:

$$\Delta\mu = \frac{1}{\beta} \frac{\text{tr} \left[\vec{\phi}_{00}^\dagger \vec{\phi}_{00} (\hat{\rho}_\phi - \hat{\rho}_{\phi, FD}(\mu_0)) \right]}{\text{tr} \left[\vec{\phi}_{00}^\dagger \vec{\phi}_{00} \hat{\rho}'_{\phi, FD}(\mu_0) \right]}, \quad (21)$$

where:

$$\hat{\varrho}'_{FD}(\mu_0) = \frac{1}{2 + e^{-\beta(H_s - \mu_0)} + e^{\beta(H_s - \mu_0)}} .$$

b. Subcase II In this subcase, we assume that both thermal smoothing and nonequilibrium modification of the distribution function corresponds to a small reciprocal vector change $\Delta\vec{k}$ compared to \vec{k}_F and all other characteristic reciprocal vectors. A somewhat cruder approximation reads:

$$\frac{1}{1 + e^{\beta(E - \mu_0 - \Delta\mu)}} - \frac{1}{1 + e^{\beta(E - \mu_0)}} \approx \delta(E - \mu_0)\Delta\mu ,$$

hence one obtains:

$$\Delta\mu = \frac{\text{tr} \left[\vec{\phi}_{00}^\dagger \vec{\phi}_{00} (\hat{\rho}_\phi - \hat{\rho}_{\phi,FD}(\mu_0)) \right]}{\text{tr} \left[\vec{\phi}_{00}^\dagger \vec{\phi}_{00} \hat{\rho}'_{\phi,FD}(\mu_0) \right]} , \quad (22)$$

where:

$$\hat{\varrho}''_{FD}(\mu_0) = \delta(H_s - \mu_0) .$$

The results above constituted a general theory of STP that is valid on all length scales and puts coherent and incoherent processes on an equal footing through the use of the density matrix. The final results from which the measured potential is implicitly determined are equations (6) or (12), which are equivalent. The result is formal, however, and not as useful as would be desirable because it requires knowledge of the density matrix over the entire sample – a formidable problem indeed. As we argue on physical grounds in the next section, some form of local density matrix would be desirable and seems possible to us, although we do not claim to provide a rigorous proof. Put more strongly, a formulation in terms of local properties will be necessary in order to make more quantitative interpretation of STP result practical.

IV. LOCAL DENSITY MATRIX

As argued above, the simple model posed here requires including both contacts providing the current and large areas of the sample that are far away from the region where STP measurement is performed, this is clearly unphysical. Moreover, the density matrix of the sample is very difficult to calculate numerically due to the large number of degrees of freedom. Equally important, ideally one would like a theory with which one can uncover relevant physics of transport without a priori knowledge of the density matrix of the sample. A proper theory in this case should only involve wave functions in the vicinity of the probed area, and involve defects and material characteristics in roughly the same area. The measurement

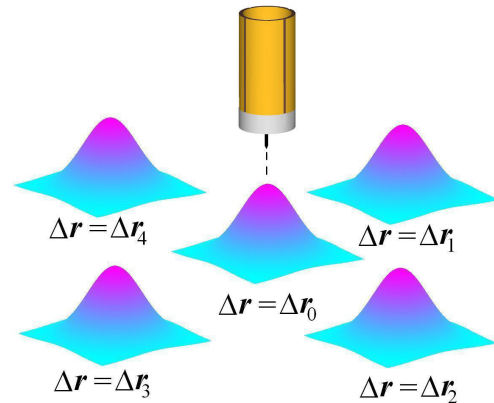


FIG. 6. Schematic of the new basis set that we propose to use in order to construct local density matrix of the sample. In this figure, only the $\Delta\vec{r}$ degree of freedom is shown. The new basis set is defined with reference to the position of the STM tip \vec{r} , with the states centered around $\vec{r} + \Delta\vec{r}_i$. The states have finite wave function values at position \vec{r} when $\Delta\vec{r}_i$ is small, and states far away with $\Delta\vec{r}_i$ large have negligible wave function values. When the position of the STM tip changes, the set $\{\Delta\vec{r}_i\}$ remains the same, hence the central locations $\{\vec{r} + \Delta\vec{r}_i\}$ changes, and the basis set changes.

result in this case should be determined by these parameters and a proper boundary condition, for example the mean current flowing near the region of the sample. We argue here that to deal with these issues it is better to describe the situation with local density matrices defined for each point on the sample, with the entries of the local density matrices consisting of only local wave functions.

A. Outline of local density matrix

Let us outline here how such a theory might be constructed. To begin, one needs electron wave functions that only extend locally. The energy eigen states that we used above to calculate the total tunneling current are extended throughout the sample, at least in the case where there are no defects in the sample. Using this basis set, all the states involved need to be counted in expression (12), because the wave functions have non-zero magnitude at the center of curvature of the tip r_0 . In order to isolate electrons far away from the measurement area, we suggest to go to other basis sets where only local wave functions are involved. In principle the density matrix of the sample is the same as when we use energy eigen states as basis states, however, a new local basis set will lead to an approximation that reduces the dimension of the density matrix, as we see below.

We propose the use of a different basis set for each point on the sample, see also Figure 6. The basis set $\{|\xi_{\vec{r} + \Delta\vec{r}_i, \vec{k}}\rangle\}$ consists of electron wave packets that are

centered around different positions $\vec{r} + \Delta\vec{r}_i$ with wave vector centered around \vec{k} . Here, the set $\{\Delta\vec{r}_i\}$ and $\{\vec{k}\}$ and the wave function forms are the same for each point, but the vector \vec{r} , which is the position where the STM tip probes, changes at different measurement positions. The matrices that are transformed from $\sum_{\vec{p}} \vec{\phi}_0^\dagger \vec{\phi}_0$ and $\sum_{\vec{p}} f(E_{c,\vec{p}} - eV_t - \mu) \vec{\phi}_0^\dagger \vec{\phi}_0$ are thus the same for different positions, except for the lateral change in \vec{r} . While being incorrect in a strict quantum mechanical context, with this new basis set, one can intuitively talk about electrons at certain positions with certain wave numbers.

Intuitively, the new basis set needs to have $\Delta\vec{r}_i$ covering the full range of the sample, in order to be a complete basis set. The matrix form of the density matrix of the sample $\langle \xi_{\vec{r}+\Delta\vec{r}_i, \vec{k}} | \hat{\rho} | \xi_{\vec{r}+\Delta\vec{r}_j, \vec{k}'} \rangle$ changes at different positions because the basis set changes.

The simplification from this approach is that density matrix elements involving wave packets far away ($\Delta\vec{r}_i$ sufficiently large) should not affect measurement result at position \vec{r} . Note that the density matrix element for these states will be finite, but because the region of finite amplitude for the wave function is far from \vec{r} , one could expect that both matrices $\sum_{\vec{p}} \vec{\phi}_0^\dagger \vec{\phi}_0$ and $\sum_{\vec{p}} f(E_{c,\vec{p}} - eV_t - \mu) \vec{\phi}_0^\dagger \vec{\phi}_0$ in equation (12) have zero elements involving these states¹⁷. With this simplification in mind, one might make an approximation and discard all states with sufficiently large $\Delta\vec{r}_i$, and reduce the problem to one that only involves electron wave packets near to the STM tip position \vec{r} . This reduced matrix form that changes with position is what we define as the local density matrix.

One could thus interpret that what STP probes in the relevant non-equilibrium conditions is the local density matrix at certain positions on the sample.

We note that if the total tunneling current was to only relate to the local density matrix at one point, the STM tip needs to be sharp, with its radius of curvature smaller than the lengthscale of variation of the local density matrix. Only in that case could one choose a surface Σ in equation (5) that is localized in space.

The concept of using basis sets with localized wavefunctions is not new, for example, codes based on linear combination of atomic orbitals (LCAO) are common in electron transport calculations^{18,19}. While using these basis sets do naturally lead to local density matrices in our notion, we would like to point out that these existing usages are mostly on small, or even molecular, samples; the calculational strategy for a proper calculation on large samples, as we will soon discuss, has not been worked out. Hence by introducing the concept of local density matrix we not only provide a theoretical convenience, but also pose a new problem in mesoscopic transport.

B. Possible further developments

The local density matrix is defined on a basis set $\{|\xi_{\vec{r}+\Delta\vec{r}_i, \vec{k}}\rangle\}$ which consists of only wave packets near to the position of STM tip \vec{r} . The matrices that are transformed from $\sum_{\vec{p}} \vec{\phi}_0^\dagger \vec{\phi}_0$ and $\sum_{\vec{p}} f(E_{c,\vec{p}} - eV_t - \mu) \vec{\phi}_0^\dagger \vec{\phi}_0$ in equation (12) are both determined by transformation rules in the Hilbert space, and, once computed, are fixed except for the position \vec{r} for different positions that the STM tip probes. In the special case described in subsection III D, the two matrices above are given explicitly by equation (17), no matter what basis set one uses.

We propose that the approach to calculate the local density matrix be different than the path of its definition. Since the local density matrix is spatially variant, there should be a controlling differential equation that determines its variation over space. One can thus pose a problem with proper boundary conditions that reflects the mean current around the probed area, and need not concern the current-providing contacts or the sample area far away from the probed area. In other words, although the derivation of the controlling equations is based on the density matrix of the sample, in the actual calculation only the local density matrix is relevant, and one does not even need to know the density matrix of the sample. The detailed form of the differential equations and boundary conditions should depend on what basis set one chooses and what further approximations one makes. We do not address these computational challenges in this paper. They require proper theorists. On the other hand, below we provide preliminary thoughts of possible further simplification procedures.

The choice of the new basis set is clearly critical in the problem. The size of the wave packets in space should be small compared to macroscopic lengths in order to make the simplification with local density matrix feasible; meanwhile this size should be large compared to λ_F , because of uncertainty principle and the need to keep the energy uncertainty small. One can thus imagine two limits to simplify the problem: one is to make relatively large wave packets, thus including more states in the local density matrix, and making the uncertainty in energy small; the other is to make relatively small wave packets, which allows to include few states in the local density matrix, but at the expense of large energy uncertainty for each basis state.

The matrices that are transformed from $\sum_{\vec{p}} \vec{\phi}_0^\dagger \vec{\phi}_0$ and $\sum_{\vec{p}} f(E_{c,\vec{p}} - eV_t - \mu) \vec{\phi}_0^\dagger \vec{\phi}_0$ in equation (12) depend on how one chooses the new basis set at each point. One can calculate these matrices according to the transformation rules, or in the case where large wave packets are adopted, one may assume that each wave packet is an approximate energy eigen state and apply these two matrices in the explicit form.

To simplify the problem without losing important information, it is reasonable to assume that all the operators $\mathcal{F}_{(\vec{p}, V_t)}$ are the same for the states in the tip as in the

special case of subsection III D, viewing the tip as part of the instrument and being controlled by the experimentalist. For example, since only nanometer scale signals are being probed, one can assume that the tip is an s -wave tip with the same constant in the matrix element calculation. This approximation was adopted in Chu & Sorbello's paper¹². Under this approximation the local density matrix approach is also better solidified.

V. LIMITING CASES

A. Sample in equilibrium

When the sample does not bear any current, i.e., is in equilibrium, after diagonalization the density matrix of

$$I = \sum_{\vec{k}, \vec{p}} \left\{ \frac{4\pi e}{\hbar} [f(E_{ec, \vec{k}} - \mu_s) - f(E_{c, \vec{p}} - eV_t - \mu_t)] \delta(E_{ec, \vec{k}}, E_{c, \vec{p}} - eV_t) \left| (\mathcal{F}_{(\vec{p}, V_t)} \psi_{\vec{k}}) |_{\vec{r}_0} \right|^2 \right\}. \quad (23)$$

Note that the Kronecker delta symbol requires the electrochemical energies for the sample state and the tip state to be the same. Under this condition and when the temperatures of the tip and the sample are the same, if $\mu_s > \mu_t$, all the terms in the above equation will be positive, hence the total tunneling current becomes positive; similarly if $\mu_s < \mu_t$, the total tunneling current becomes negative. The only possibility for the total tunneling current to be zero is if $\mu_s = \mu_t$, regardless where the tip is. This is expected from physical consideration. When the temperatures of the tip and the sample are different, the above conclusion is no longer true, but this is expected as a thermal electric effect.

B. Homogeneous sample with no defect

Suppose the sample does not have any defects, namely, there is only inelastic scattering and no elastic scattering in the sample. Also suppose that the current is uniform on the sample. In a jellium model, from translational symmetry of the sample (neglecting effects due to the macroscopic contacts), one expects that the local density matrix should be the same throughout the probed area, except for the effect from a linear electrostatic potential distribution reflecting the fact that there is a constant current and there exists inelastic scattering. In this case, the local density matrix is described by a distribution function (no off-diagonal elements), because electrons at different eigen states are incoherent to each other. In the linear response limit, the distribution function reads:

$$f(\vec{k}, \vec{r}) \propto \frac{1}{e^{\beta(E_{\vec{k}} - \mu_{\hat{\theta}, \vec{r}})} + 1}$$

the sample will become a Fermi-Dirac distribution, i.e., suppose the basis set $\{|\psi_{\vec{k}}\rangle\}$ diagonalizes $\hat{\rho}$, one obtains from equation (6):

$$\mu_{\hat{\theta}, \vec{r}} = e\vec{E} \cdot \vec{r} + \mu - el_{in}\vec{E} \cdot \hat{\theta}. \quad (24)$$

For each direction of momentum there exist an effective chemical potential $\mu_{\hat{\theta}}$. This distribution function leads to the distribution function with electrochemical energy as a variant in equation (2). In this case, in STP measurement the difference of data at different points comes from the $-\vec{E} \cdot \vec{r}$ term.

C. Landauer resistive dipole

Suppose there is only one defect on the otherwise homogeneous sample, or assume the defects are far away from each other compared to l_{in} . Far away from the defect(s), electrons are not coherent to one another due to inelastic scattering events after they are reflected by the defect(s). At these positions, the local density matrix will again be described by a distribution function. In the linear response limit, the distribution function will be very similar to equation (24) above, namely:

$$f(\vec{k}, \vec{r}) \propto \frac{1}{e^{\beta(E_{\vec{k}} - \mu_{\hat{\theta}, \vec{r}})} + 1}$$

$$\mu_{\hat{\theta}, \vec{r}} = -e\phi(\vec{r}) + \mu + el_{in}\nabla\phi \cdot \hat{\theta}, \quad (25)$$

where $\phi(\vec{r})$ is the Landauer resistive dipole potential¹³. This demonstrates that STP can measure the Landauer resistive dipole potential, which is expected from physical consideration. Resistive dipoles have been observed by experiments². Equations (24) and (25) are similar to each other, because at the regions where Landauer derived

the resistive dipole, the only practical difference is that the electrostatic potential is different than the previous limiting case due to the existence of the scattering center. Here $\phi(\vec{r})$ is the dipole field plus the homogeneous electric field.

D. Chu and Sorbello model

Chu and Sorbello¹² calculated the STP measurement result much nearer to a defect than l_{in} . In the paper it is assumed that the electrons have a specific distribution function in \vec{k} space before encountering the scattering center, and after being deflected by the scatterer, the electrons are not deflected again by the same scatterer. Interpreting their calculation in our context, they view most part of the sample as the current-providing electrodes that inject the incoming electrons with the specific distribution into the “sample”, and the sample size is effectively much smaller than l_{in} , centering around the defect. Once the electrons enter the sample they remain coherent in the presence of elastic scattering. The reservoir case, the background scatterers case and the semi-classical barrier case are all describing the distribution of the injected electrons. In our context, the density matrix of the sample, which is only a very small region near the defect, is completely known:

$$\varrho = \sum_{\vec{k}} f(\vec{k}) \left| \psi_{\vec{k}}^{(+)} \right\rangle \left\langle \psi_{\vec{k}}^{(+)} \right|, \quad (26)$$

here $\left| \psi_{\vec{k}}^{(+)} \right\rangle$ is the purely coherent state resulting from one channel of injected electron from the contacts.

If one considers the case where the part of the sample that is not close to the defect is also measured by STP, the above density matrix no longer describes the situation, that is to say, equation (26) does not describe all the electrons in the system. However, it is conceivable that with a local density matrix description, the local density matrix very near the defect does look like equation (26).

Using equation (22) and noticing that $f(E_{\vec{k}} - \mu_{\vec{k}}) - f(E_{\vec{k}} - \mu) \approx \delta(E_{\vec{k}} - \mu)(\mu_{\vec{k}} - \mu)$, one obtains:

$$\delta V_{STP}(\vec{r}_0) = \frac{1/e \sum_{\vec{k}} |\psi_{\vec{k}}^{(+)}(\vec{r}_0)|^2 \delta(E_{\vec{k}} - \mu)(\mu_{\vec{k}} - \mu)}{\sum_{\vec{k}} |\psi_{\vec{k}}^{(+)}(\vec{r}_0)|^2 \delta(E_{\vec{k}} - \mu)}, \quad (27)$$

which is equation (14) in Chu and Sorbello’s paper. This illustrates the reason why tunneling matrix elements should not be assumed to have the same magnitude in writing down the total tunneling current, as the variation of this magnitude is the interference term. It can also be seen from this expression that the density matrix of the sample determines how and where this variation occurs.

E. Atomic resolution in STP

As we have emphasized, the tunneling matrix elements are dependent on electron wave function values, which change over space, leading to the quantum interference effects in the end result of STP. In normal STM mode, it is also the change of tunneling matrix elements within a unit cell that leads to atomic resolution of STM (and practically, in order that the atomic corrugations be measurable, the tip should usually be sharper than an s-wave tip, i.e., the operators \mathcal{F} acting on the wave functions should not be as simple as a pure number, see also discussions in Chapter 7 of reference 14). It is then natural to ask the following question: does there exist atomic resolution (i.e., corrugations in the end result due to wave function value changes within a unit cell) in STP measurements?

Part of the answer to the previous question is simple. As we discussed in the first limiting case in this section, without a current (sample in equilibrium), there shall be atomic resolution in STM, but one will see no atomic corrugation in STP measurement because it is a constant throughout the sample. This demonstrates that if there is atomic resolution in STP, it should be different in origin than atomic resolution in STM mode. The answer to this question when there is a current on the sample becomes complicated. To demonstrate the nature of this problem, we investigate the STP measurement on a simple toy model, namely a one-dimensional tight-binding model with only one atomic orbital involved. Readers are referred to Chapter 10 of reference 20 for the basic setup of tight-binding model.

We assume that the sample is one dimensional and is well described by a tight-binding model with only one atomic orbital, the wave function of which is $\phi(x)$. $\phi(x)$ is centered around $x = 0$. The lattice constant of the sample is a . In the tight-binding model, the wave functions of the band is known:

$$\psi_k(x) = \sum_n e^{ikna} \phi(x - na), \quad (28)$$

where $k \in (-\frac{\pi}{a}, \frac{\pi}{a})$, which is the first Brillouin zone. For our purpose, it suffices to assume that $\phi(x)$ is a s-level and to use nearest neighbor approximation, which lead to the band structure:

$$E(k) = E_0 - \gamma \cos(ka), \quad (29)$$

where E_0 and γ are two numbers related to the s-level energy and $\Delta U(x)$ which is the correction to the atomic Hamiltonian. To further simplify things, we assume that all operators \mathcal{F} are the same for all states (i.e., approximation(14) stands, and the expression for total tunneling current is equation (19)) for now.

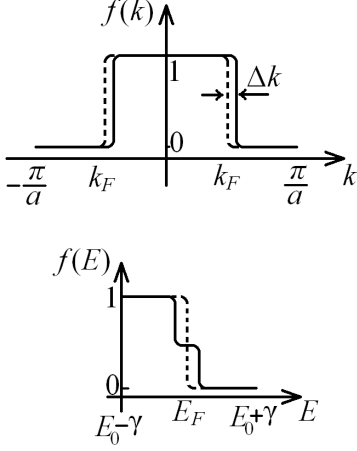


FIG. 7. Sketch of distribution function with respect to k (upper panel) and E (lower panel), both without current (dashed lines) and with a current (solid lines), in the tight-binding model without defects under consideration.

1. Sample with no defects

Suppose the sample has no defects, then the density matrix of the sample is diagonal under the basis of $\{\psi_k\}$. We can use a distribution function $f(k)$ to describe things, and the distribution function with respect to energy $f(E)$ can be calculated from $f(k)$. If we ignore the thermal broadening, the distribution function with respect to both k and energy is sketched in Figure 7.

$$\begin{aligned}
 I \propto \sum_k |\mathcal{F}_0\phi(x_0) + e^{ika}\mathcal{F}_0\phi(x_0 - a)|^2 (f(k) - f_{FD}(k, \mu)) &= \left(|\mathcal{F}_0\phi(x_0)|^2 + |\mathcal{F}_0\phi(x_0 - a)|^2\right) \sum_k (f(k) - f_{FD}(k, \mu)) \\
 + \sum_k [(\mathcal{F}_0\phi(x_0))^* \mathcal{F}_0\phi(x_0 - a)e^{ika} + \mathcal{F}_0\phi(x_0) (\mathcal{F}_0\phi(x_0 - a))^* e^{-ika}] (f(k) - f_{FD}(k, \mu)) . & \quad (32)
 \end{aligned}$$

It is reasonable to assume that $(\mathcal{F}_0\phi(x_0))^* \mathcal{F}_0\phi(x_0 - a)$ is real, then the second line of equation (32) equals:

$$2(\mathcal{F}_0\phi(x_0))^* \mathcal{F}_0\phi(x_0 - a) \sum_k \cos(ka) (f(k) - f_{FD}(k, \mu)) . \quad (33)$$

When the current in the sample is small and the system is in linear response region, and if μ is the value that makes the first line of equation (32) zero, then the range of k for nonzero $[f(k) - f_{FD}(k, \mu)]$ values consists of two very narrow regions centered around $-k_F$ and k_F , and because $\cos(k_F a) = \cos(-k_F a)$, expression (33) equals

The total tunneling current in this case reads:

$$I = \frac{4\pi e}{\hbar} N_t \cdot \sum_k |\mathcal{F}_0\psi_k(x_0)|^2 (f(k) - f_{FD}(k, \mu)) , \quad (30)$$

where $f_{FD}(k, \mu)$ is the Fermi-Dirac distribution function with chemical potential μ (dashed curve in lower panel of Figure 7 but has a freedom to move in the horizontal direction depending on the value of μ). The question then becomes: does the value of μ that makes equation (30) equal to zero have a spatial dependence (as x_0 changes within the unit cell)?

a. x_0 close to origin When we consider the STP measurement results in the vicinity of the atomic orbital, only the $n = 0$ component in the definition of $\psi_k(x)$ in equation (28) is relevant, thus the total tunneling current becomes:

$$\begin{aligned}
 I &\propto \sum_k |\mathcal{F}_0\phi(x_0)|^2 (f(k) - f_{FD}(k, \mu)) \\
 &= |\mathcal{F}_0\phi(x_0)|^2 \sum_k (f(k) - f_{FD}(k, \mu)) . \quad (31)
 \end{aligned}$$

Hence there is no spatial dependence in μ . This is in contrast to atomically resolved corrugations in STM mode, in which case the change in $|\mathcal{F}_0\phi(x_0)|^2$ indicates a spatial change in the measured sample height.

b. x_0 close to $a/2$ Now consider the case where the probed point is not close to the vicinity of the atomic orbital, i.e., at least two (and in nearest neighbor approximation we consider only two, for example $n = 0$ and 1) components in equation (28) should be considered. The total tunneling current then reads:

zero, too. In other words, to this order there is still no spatial dependence in the measured STP potential.

If the current in the sample is large enough, such that Δk in Figure 7 is significant, then the above argument breaks down and there will be a small corrugation in measured STP potential in the atomic resolution.

2. Sample with defect(s)

When the sample does have defect(s), under the basis $\{\psi_k\}$ the density matrix of the sample has off-diagonal elements. As we do not address the calculation of the density matrix, we only consider the case in which there is one off-diagonal element between states k_0 and $-k_0$ (degenerate states and k_0 is close to k_F). Suppose the off-diagonal element is δ in the $(k_0, -k_0)$ entry of the density matrix, and δ^* in the $(-k_0, k_0)$ entry. One only needs one additional term in equation (31) or (32) in this case:

$$\Delta I = \mathcal{F}_0 \psi_{k_0}(x_0) (\mathcal{F}_0 \psi_{-k_0}(x_0))^* \delta^* + \text{complex conjugate} \quad (34)$$

With the same assumption above for the defect-free case that $\mathcal{F}_0 \psi_{k_0}(x_0) (\mathcal{F}_0 \psi_{-k_0}(x_0))^*$ is real, we arrive at:

$$\Delta I = 2\mathcal{F}_0 \psi_{k_0}(x_0) (\mathcal{F}_0 \psi_{-k_0}(x_0))^* \text{Re}(\delta) \quad (35)$$

a. x_0 close to origin In this case, equation (31) becomes:

$$\sum_k (f(k) - f_{FD}(k, \mu)) + 2\text{Re}(\delta) = 0 ,$$

hence there is no spatial dependence in μ .

b. x_0 close to $a/2$ In this case, the correction to equation (32) includes a term:

$$2\text{Re}(\delta) (\mathcal{F}_0 \phi(x_0))^* \mathcal{F}_0 \phi(x_0 - a) \cos(k_0 a) \\ \times (f(k_0) - f_{FD}(k_0, \mu)) ,$$

which does lead to a spatial dependence in μ which is proportional to δ .

To sum up, when there are static defects in the sample, in the transition region between two adjacent atomic sites, there will be atomically resolved corrugations due to changes in wave function values, but this corrugation is a second order effect, as opposed to the first order effect in STM mode. If the sample does not have defects, hence no interference between states, the atomic corrugation is an even higher order effect.

Though the above results are obtained in a simplified toy model, we believe the conclusion bears some universality. It also demonstrates the nature of the STP potential problem, in that to first order the results are often trivial, in order to manifest effects from either wave function value changes or quantum interference, one often needs to go to a higher order. This is also part of the reasons that we are not able to provide estimates of the size of these effects without calculating the actual density matrices.

VI. SUMMARY AND DISCUSSION

In this paper, we developed a viewpoint of STP measurement in the framework of quantum transport. Equation (12) gives an expression of the total tunneling current which is dependent on the distribution function of

the STM tip and the density matrix of the sample. By setting this total tunneling current zero, one implicitly determines the STP measurement result. The expression is in a matrix product form such that a basis-set free definition can be made. With some approximations, we also obtained explicit expressions for measured STP potential in the featureless tip case.

In order to get rid of the unphysical requirement of material characteristics far away from the STP probing area in writing down the density matrix of the sample, we proposed to use local density matrices, defined in Section IV, as a varying parameter over space, which is controlled by a certain differential equation and a set of boundary conditions. This allows relating STP to sample properties near the region where STP is performed.

In Section V we provided limiting case calculations that demonstrate the usage of the theoretical description, mostly with given or assumed density matrices of the sample. In particular, we found that with the toy model of one dimensional tight-binding metal, atomic resolution in STP measurement is a high order effect. Following the derivation of this particular example, one can find that the null results are partly due to assumed symmetry in the Fermi surface (e.g., Equation (33) being zero under the adopted assumptions) or in the operators \mathcal{F} acting on the sample wave functions. We speculate that asymmetry in the Fermi surface with respect to \vec{k} , or in the tip wave function (hence operator \mathcal{F}) with respect to energy, could lead to lower order effects in STP measurement.

Comparing equation (12) with, for example, equation (8.6.6) in reference 15, one can immediately see the analogy. The matrices $\sum_{\vec{p}} \vec{\phi}_0^\dagger \vec{\phi}_0$ and $\sum_{\vec{p}} f(E_{c,\vec{p}} - eV_t - \mu) \vec{\phi}_0^\dagger \vec{\phi}_0$ are in the same place where the scattering matrices are. Although one needs to keep the subtle difference between correlation function and density matrix in mind, these two matrices can be viewed as a special kind of scattering matrix.

The STM tip as a special contact provides scattering which is described by a scattering matrix related to the matrices mentioned above. This implies that it will also act as an electron source, the strength of which is dependent on the strength of scattering. The electron source effect will change the density matrix of the sample, or the local density matrix, as the tip moves. However, in the limiting case that the strength of scattering is small, i.e., the probe is weakly interacting with the sample, STP measurement result is not expected to change much. STP does have this advantage of perturbing the sample minimally, compared to other contact-based probes, for example, using conducting cantilevers as the fourth electrode and using an atomic force microscope to scan on the sample. Conceptually, a good criteria for minimal source effect would be that the tip should be far away from the sample that it is in the far tail of the exponential decay of electron wave function for sample states, though this will correspond to a large tunneling resistance and the resolution of the STP measurement in this case is expected

to be low due to large Johnson noise. Nevertheless, it is a valid starting point to work under this assumption to simplify the problem. When the sample is small compared to its characteristic transport lengths, the effect of the tip is generally large and these effects are already explicitly included in the formalism of works on this case^{7,8}.

ACKNOWLEDGMENTS

We would like to thank Supriyo Datta and Kirk H. Bevan for a critical reading of the original draft of this manuscript and their valuable comments and suggestions. Support for this work came from the Air Force Office of Scientific Research. One of us (WW) further acknowledges the generous support of a Stanford Graduate Fellowship.

-
- * weigwang@stanford.edu
- ¹ P. Murali and D. W. Pohl, *Applied Physics Letters* **48**, 514 (1986).
 - ² B. G. Briner, R. M. Feenstra, T. P. Chin, and J. M. Woodall, *Physical Review B* **54**, R5283 (1996).
 - ³ M. Rozler and M. R. Beasley, *Review of Scientific Instruments* **79**, 073904 (2008).
 - ⁴ A. Bannani, C. A. Bobisch, and R. Moller, *Review of Scientific Instruments* **79**, 083704 (2008).
 - ⁵ J. Homoth, M. Wenderoth, T. Druga, L. Winking, R. G. Ulbrich, C. A. Bobisch, B. Weyers, A. Bannani, E. Zubkov, A. M. Bernhart, M. R. Kaspers, and R. Moller, *Nano Letters* **9**, 1588 (2009).
 - ⁶ T. Druga, M. Wenderoth, J. Homoth, M. A. Schneider, and R. G. Ulbrich, *Review of Scientific Instruments* **81**, 083704 (2010).
 - ⁷ T. Gramspacher and M. Buttiker, *Physical Review B* **56**, 13026 (1997).
 - ⁸ T. Gramspacher and M. Buttiker, *Physical Review B* **60**, 2375 (1999).
 - ⁹ T. Todorov, *Philosophical Magazine B* **79**, 1577 (1999).
 - ¹⁰ Y. Q. Xue and M. A. Ratner, *Physical Review B* **70**, 081404(R) (2004).
 - ¹¹ Y. Xue and M. Ratner, *International Journal of Quantum Chemistry* **102**, 911 (2005).
 - ¹² C. S. Chu and R. S. Sorbello, *Physical Review B* **42**, 4928 (1990).
 - ¹³ R. Landauer, *Ibm Journal of Research and Development* **1**, 223 (1957).
 - ¹⁴ C. J. Chen, *Introduction to scanning tunneling microscopy*, 2nd ed., Monographs on the physics and chemistry of materials (Oxford University Press, Oxford ; New York, 2008).
 - ¹⁵ S. Datta, *Electronic transport in mesoscopic systems*, Cambridge studies in semiconductor physics and microelectronic engineering (Cambridge University Press, Cambridge ; New York, 1995).
 - ¹⁶ Formally, to include all the information one needs to use correlation functions which also give the phase difference between states at different time, whereas as we show below, the density matrix of the sample which only specifies phase difference between states at the same time is sufficient to describe the situation.
 - ¹⁷ This is obtained from physical intuition, which needs to be verified once the basis set is chosen. In fact, the intuition that zero wave function value implies zero tunneling current comes from energy eigen states, but the new basis set does not consist of energy eigen states in the strict sense. In the special case discussed in subsection III D with a featureless tip, this physical intuition is formally proven.
 - ¹⁸ W. Cheng, Y. Liao, H. Chen, R. Note, H. Mizuseki, and Y. Kawazoe, *Physics Letters A* **326**, 412 (2004).
 - ¹⁹ B. Wang, Y. Zhu, W. Ren, J. Wang, and H. Guo, *Physical Review B (Condensed Matter and Materials Physics)* **75**, 235415 (2007).
 - ²⁰ N. W. Ashcroft and N. D. Mermin, *Solid state physics* (Philadelphia: Saunders College, 1976).